

CAVITATION EROSION PREDICTION FROM INFERRED FORCES USING MATERIAL RESISTANCE DATA

Xavier Escaler[†], François Avellan[‡], Eduard Egusquiza[†]

[†] Technical University of Catalonia (UPC), Barcelona, SPAIN

[‡] Swiss Federal Institute of Technology (EPFL), Lausanne, SWITZERLAND

Abstract

To improve cavitation erosion prediction based on induced vibrations, some experimental work has been carried out on two different materials, a stainless steel and a protective coating. First, the erosive characteristics of the materials have been analyzed in a cavitating vortex generator. Pit counting results have been correlated to inferred force intensities occurring on the eroded area from measured vibrations considering the transmissibility from the excitation location to the measuring position. The relationship between the pit area and the force intensity has been calculated. To validate these results, the same materials have been tested in a hydrodynamic tunnel where the force intensities have been inferred in the same way. Then, the eroded area has been calculated using the erosion characteristics previously determined. The results obtained compare well with the actual erosion measured on the tunnel specimens. Next step is to apply this method to hydraulic machines.

1 Introduction

The most promising methodologies to predict cavitation erosion of materials in hydraulic machines are based on the measurement of cavitation induced vibrations (see for example, Kaye 1999 and Bourdon 2000). Although satisfactory results have been recently obtained with these methods, they are incomplete because the material characteristics are not taken into account and the transmissibility characteristics between the source of excitation and the measuring position are not well known.

Actually, no absolute method to quantify cavitation erosiveness has been fully validated from a practical point of view so that it can be successfully applied to hydraulic machines or systems. One of the lacking points is that the specific resistance of the material forming the solid surface that receives the impact forces is not taken into account. Therefore, it would be convenient to consider the intrinsic material resistance to the cavitation attack since materials of different nature might have significantly different responses when submitted to the same level of cavitation aggressiveness.

The aim of the current work has been to define a more complete approach to the problem. The first step of the method consists in determining the erosive characteristics of the materials versus the force intensity of a vortex cavity collapse. Then, this information can be used to estimate the erosion rate from the inferred force intensities acting on the eroded area in any other cavitating system. The intensity of cavitation can be estimated from vibration measurements taking into account the transmissibility from the excitation to where vibration is measured.

The proposed method uses erosion results obtained in a vortex generator to determine the resistance of a material against cavitation erosion. This is done by correlating absolute collapse forces with the area of the resulting pits, as presented in Escaler *et al.* (1999). Then, the validity of these results to predict cavitation erosion is checked in a hydrodynamic tunnel. The tunnel can reproduce hydrodynamic conditions closer to what is encountered in actual water turbines. Particularly, the investigation is carried out with two materials of different nature, a stainless steel and a protective coating.

The ultimate application of such results is aimed to improve the existing on-line cavitation erosion monitoring systems for prototypes so that the erosion rate could be estimated with a better accuracy.

2 Experimental Setup and Methods

2.1 Testing Devices

The *Vortex Cavitation Generator (VCG)* of IMHEF-EPFL is a closed loop that allows performing erosion tests on cylindrical specimens with a diameter of 11 mm, flush mounted in the test section. The working principle is to produce, at every revolution of a rotating valve, the growth and collapse of a vapor cavity in a vortex flow field. The collapse overpressure endured by the specimen may reach several GPa (Farhat and Avellan, 1988). The resulting cavitation pits on ductile materials are found to be similar to those produced by travelling cavities downstream an attached leading edge cavity (Karimi and Avellan, 1986).

The *High-Speed Cavitation Tunnel* of IMHEF-EPFL has a test section of $150 \times 150 \times 750 \text{ mm}^3$ (Avellan *et al.*, 1987). The maximum inlet flow velocity is 50 m/s. The operating parameters, namely flow velocity and sigma value, are automatically regulated to ensure steady conditions in the test section. A 2D plane-convex hydrofoil of 100 mm chord length and 150 mm span has been used (Quang, 1984). The profile cross-section has a flat suction side and a circular pressure side of 110.2 mm radius. Its maximum thickness is 12 mm. Up to 4 rectangular samples, having a flat exposed surface of $25 \times 81.1 \text{ mm}^2$, can be bolted to the hydrofoil. Four identical semi-cylinders with a height of 10 mm and a diameter of 5 mm have been mounted on the profile leading edge as shown on Figure 1. The purpose of using the obstacles has been to alter the flow field on the suction side in order to accelerate the erosion process. Prior to the erosion tests, four different obstacles have been tested in order to determine the most adequate geometry and dimensions. The semi-cylindrical obstacle has been proved to be the best one for generating reproducible pitting on the specimen in a relatively short period of time as described in Escaler (2000).

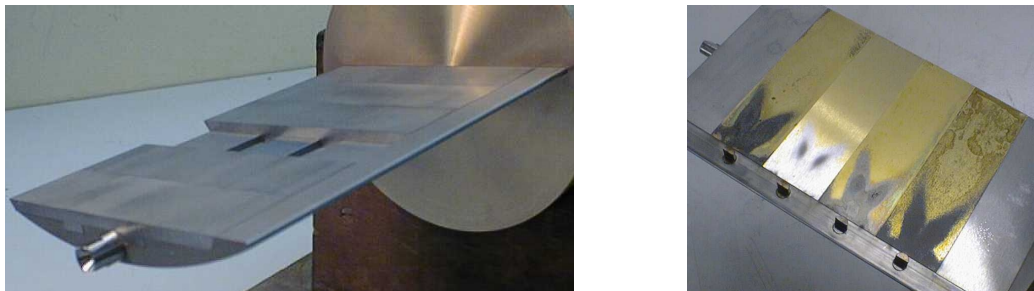


Figure 1: Left: Lateral view of the plane-convex hydrofoil. Right: Top view of the hydrofoil with the obstacles and the eroded specimens at the end of the tests.

2.2 Tested Materials

A stainless steel X5 Cr Ni 13.4. and a thermal spray coating which is tungsten carbide based have been used for the tests. The materials are named in the text as REF and E, respectively. A brief description of their composition is indicated in Table 1.

Material		Composition-Nature		
REF	Metal	Ductile	Wrought	Dense
E	Cermet	Semi-Ductile	Sprayed	Low Porosity

Table 1: Comparison of the composition and nature for the tested materials

2.3 Erosion Tests

In the VCG, the erosion tests have consisted in submitting the material to a series of repetitive single vapor cavity collapses at a constant rate in order to obtain enough pitting without overlapping. For material REF

the total duration of the tests has been 109 minutes. For material E the total duration has been 42 minutes. In both cases, the operating conditions have been kept the same.

In the Hydrodynamic Tunnel, the materials have been tested in two identical runs of 75 *h* each with the plane-convex hydrofoil equipped with the semi-cylindrical obstacles. The flow velocity has been set to 35 *m/s*, the sigma value to 1 and the incidence angle to 3°. Flow visualizations of the cavitation generated behind the obstacles are presented on Figure 2.

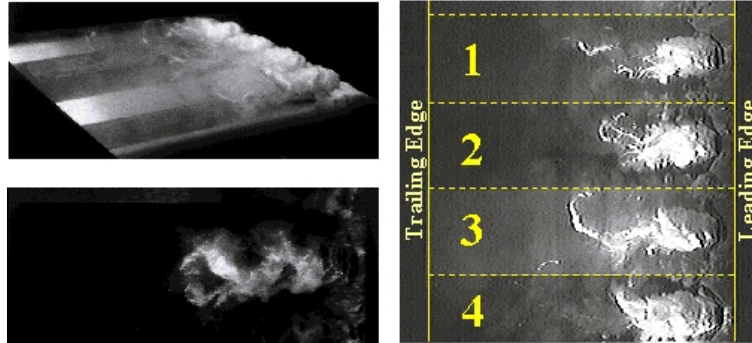


Figure 2: Flow visualizations of the cavitation generated behind the obstacles at a flow velocity of 35 *m/s*, a sigma value of 1 and an incidence angle of 3°.

The runs have not been carried out continuously but in intervals of about 10 *h*, since the tunnel had to be stopped during the night for safety reasons. Performing two runs have permitted to check the test reproducibility and the influence of sample position. The hydrodynamic parameters of the cavitation tunnel have been continuously monitored during the tests and the values of flow velocity, sigma, incidence and water temperature have confirmed the similarity of the tests. In the first run the two central positions on the blade have been used to test the specimens of each material simultaneously. In the second run the specimen positions have been interchanged. A thin layer of gold (few nanometers) had been applied to the wear specimens on the exposed surface before the tests in order to facilitate the localization of the zone of cavitation attack during the initial stages of damage.

2.4 Signal Acquisition System

The output signals from the vibration sensors have been recorded with an analogue to digital 12-bit waveform recorder LeCroy 6810. The recording is always initiated by a trigger that can be set to meet specific waveform conditions or done by software. A channel signal can act as the trigger source. In addition, the 6810 records the trigger-to-trigger times from segment to segment which helps to precisely reconstruct the timing of intermittent waveforms. The stored data is then transmitted to the PC acquisition system through a GPIB port using the CAMAC interface module LeCroy 6010.

In the VCG, the sample holder has been equipped with the shock accelerometer Brüel&Kjær type 8309 with integral mounting stud and a mounted resonance frequency of 180 *kHz*. This vibration sensor is conditioned with a charge amplifier B&K 2650 with a linear filter from 3 *Hz* to 200 *kHz*. A sampling frequency of 500 *kHz* has been used for signal recording.

In the Hydrodynamic Tunnel, vibrations have been measured by means of a miniature piezoelectric accelerometer type Kistler 8614A500M1 with a measuring range of ± 500 *g* and a theoretical mounted resonant frequency of 125 *kHz*. The transducer has been glued externally to the test section in the hydrofoil bedplate flange. The output signal has been band-pass filtered between 2 and 100 *kHz* for noise reduction and anti-aliasing. A sampling frequency of 200 *kHz* has been used for signal recording.

2.5 Dynamic Calibration

The dynamic calibration assumes that the structural response to an external excitation is governed by a linear and time invariant Frequency Response Function (FRF). The method used to determine the FRF of the physical system consists in applying an artificial excitation with a miniature-instrumented hammer

DYTRAN 5800SL and measuring the response with the vibration sensor. The technical specifications of the hammer are a reference sensitivity of $99.8 \text{ mV/Lb.} - F$, a range of $50 \text{ Lb.} - F$ and a resonant frequency of 300 kHz .

The calibration in the VCG has been carried out at the completion of the tests with the sample mounted on an external setup without water (Figure 3), almost identical to the vortex tube closed end. This method has been used because the test section is not accessible in the operating configuration. Therefore, the water added mass effect, which exists in the actual operation, is not simulated. The FRF is determined between the specimen's surface and the accelerometer in its measuring position.

In the Hydrodynamic Tunnel, the FRF between the hydrofoil suction side and the external measuring point has been estimated with the same hammer used for the VCG. The hammer impacts have been applied at the end of the erosion tests. In this particular case, the influence of the added mass effect and the location of the excitation has been considered due to the larger size of the system. On the one hand, the hydrofoil has been partially submerged leaving the upper half of the tunnel test section empty of water (see Figure 3). Then, the hammer impacts have been applied to the upper side of the profile. On the other hand, it has been considered the fact that the implosions happening farther to the measuring location generate a lower response than the ones that occur much closer. As a solution, it has been proposed to average the results inferred from two FRF's obtained from extreme positions. The materials of interest have been kept safe and only the lateral samples indicated on left of Figure 4 have been used for calibration. In the same Figure 4 the resulting response functions from each side of the blade are plotted. The 'FRF 1 close' quantifies the response of the accelerometer to an impulsive excitation occurring next to it and 'FRF 2 far' to another one occurring far from it. It must be noted that differences in gain are observed between them.

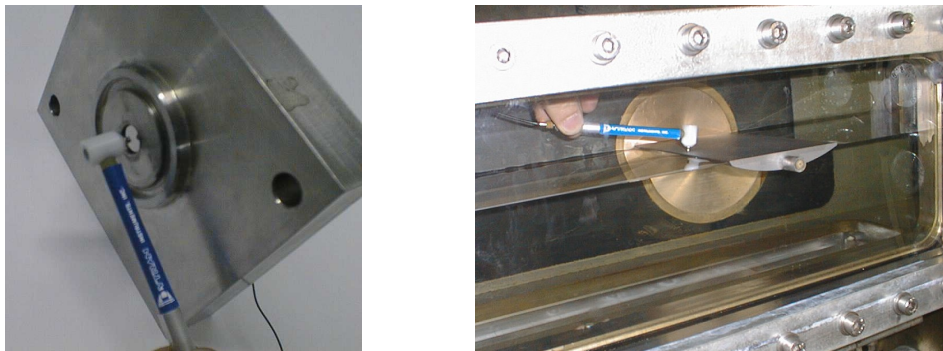


Figure 3: Calibration procedure in the Vortex Generator (Left) and in the Hydrodynamic Tunnel (Right).

Consequently, both frequency response functions have been considered to infer the maximum and the minimum force values that could be responsible for a given impulsive response measured during the tests. The average value from the two results has been considered for further analysis. This value corresponds to the equivalent force level that should be applied to the center of the blade in order to generate the measured response.

2.6 Pit Counting and Mass Loss

Pit counting has been carried out in the VCG. Pits due to cavitation have been determined using an image processing method presented in Escaler *et al.* (1999) from pictures of the sample surface taken before and after the tests.

The profiles of the eroded surfaces in the Hydrodynamic Tunnel have been measured in two perpendicular directions with a non-contact surface profilometer (UBM) and the relative volume loss has been calculated from the 2D profile wear measurements.

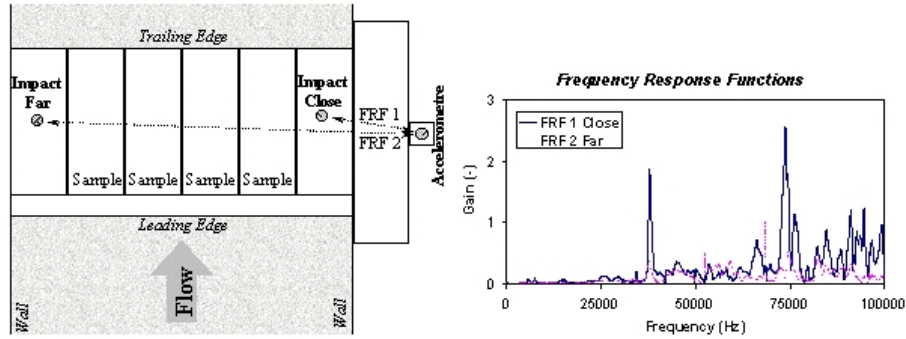


Figure 4: Left: Schematic representation of the two impact positions on the hydrofoil during calibration. Right: Resulting frequency response functions from the two positions.

3 Results

3.1 Material Resistance Data from VCG

The tests have been carried out with the aim of evaluating the erosion characteristics of the two materials and to quantify their resistance in terms of pit area against force level inferred from cavity collapse induced vibration. The tests have involved a short series of single vortex collapse impacts applied to the specimens until enough pitting has been generated without overlapping. During the tests, the shock vibrations induced by the collapses have been recorded. Due to the variability and the randomness of the impact forces, a trigger has been set in such a way that only the collapses exceeding a certain level of acceleration have been stored. The acquisition parameters have been a sampling frequency of 500 kHz , a time length for each data segment of $0,004096\text{ s}$ (2048 samples). The absolute accelerations have been low-pass filtered below 200 kHz . The corresponding forces have been inferred for each material by means of its frequency response function and the maximum force levels have been considered. The area of the pits occurred during the tests has been measured from surface pictures taken with an optic microscope. The pits have been selected comparing the surface before and after the tests. As a result, it has been possible to establish a direct correlation between the maximum values of the impact forces and the pit areas, and to estimate a damaging threshold above which damage appears. On Figure 5, the relation between pit areas and impact forces are compared for materials REF and E. Table 2 indicate the linear regressions that fit the data and the damaging thresholds that result from them. For detailed information about these particular results see Escaler (2000).

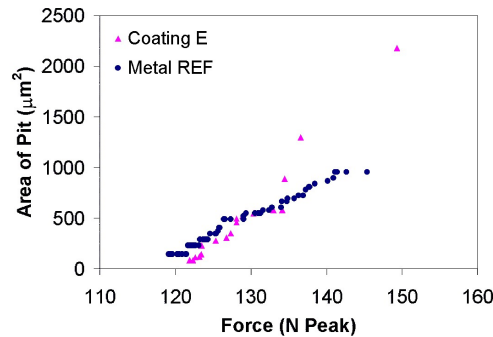


Figure 5: Comparison of correlations between maximum values of inferred forces and resulting pit areas for materials REF and E.

Material	Regression (Pit area mm^2 ; Force N)	Damaging Threshold (N)
REF	Pit area = $35.6 \times F - 4114.8$	115.6
E	Pit area = $73.4 \times F - 8939.7$	121.8

Table 2: Linear regressions and damaging thresholds for materials REF and E obtained in the VCG.

3.2 Inferred Forces from Hydrodynamic Tunnel

Cavitation induced vibrations have been monitored during the laboratory tests in the hydrodynamic tunnel. The intensity of the cavitation attack has been evaluated with the statistical analysis of the maximum values of the inferred forces. Two different types of measurements have been devised with the purpose of investigating the nature and characteristics of the cavitation generated on the specimens.

On the one hand, the *continuous measurements* have consisted in the record of time segments of about 5.2 s length in order to have an idea of the overall trends of vibration intensity at various instants during the test. These measurements have usually been carried out at the beginning and at the end of a test period. On the other hand, the *triggered measurements* have consisted in a continuous and selective acquisition of short data samples (250 segments of about 0.02 s each) containing the most powerful impulses appeared during a test period. In this way, it has been possible to characterize the most significant incidences occurred during the 75 h. Histogram type plots have been used to analyze the statistical distribution of the transient events occurred during one of the runs.

The impulsive vibrations monitored with the *triggered measurements* have been quantified considering the maximum value for each segment of recorded data. For the long data segments obtained with the *continuous measurements* a post-processing method based on a digital threshold peak detector has been used to extract short data batches (0.02 s) containing significant pulses. By using an adequate threshold level, the peaks have been detected and quantified as the former. Thereby, analogous histogram plots have been obtained from both types of measurements, which allows for comparison.

An estimation of the total distribution of inferred force values for a complete test (75 h) has been done using the production rate data obtained from the second run measurements. For the *triggered measurements*, a total of 2144 events have been selected with a trigger level of 216.6 g during a time period of approximately 67 h. For the *continuous measurements*, a total of 4868 events have been selected with a trigger level of 89.2 g during a time period of approximately 4.3 minutes. The corresponding histogram of maximum force values estimated for one specimen during 75 h is shown on Figure 7. As it can be observed, the strongest impacts occur below 1200 N. The most powerful impacts are few compared to the enormous concentration of lower energy impacts.

3.3 Mass Loss from Hydrodynamic Tunnel

At the completion of the 75 h, the samples present material loss as it can be observed on Figure 1. The wear is mainly located in two elliptical and symmetric areas in the upstream half of the surface, immediately behind the obstacle for all the specimens. Cavitation erosion is strongly concentrated in the center of each region and diminishes gradually towards the border. In the downstream half of the samples, few isolated impacts of big sizes are also observed widely scattered. The region where collapses take place appears gradually from the first hours and no sudden increase of damage is observed during the run. On Figure 6, enlarged pictures of the eroded regions on the specimens at the end of the tests are shown.

The relative volume loss has been calculated from 2D profile wear measurements conducted on the specimens (Table 3). A low dependency of the final erosion on sample position is confirmed because the two materials exhibit similar levels of mass loss independently of their position on the hydrofoil.

4 Discussion

Figure 5 shows the area of the resulting pit as a function of the maximum amplitude of the inferred force due to the vortex cavity collapse for the two materials. At first glance, it can be observed that the linear regression corresponding to each material intersect with each other. Actually, this behavior indicates that

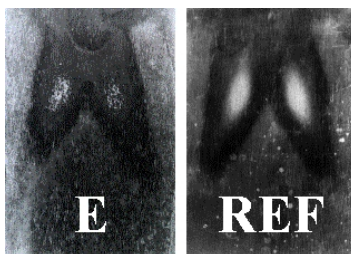


Figure 6: Pictures of the erodes regions at the completion of the tunnel tests for materials REF and E.

Material	Relative Volume Loss
REF	12
E	70

Table 3: Averaged relative volume loss measured on the specimens after 75 h in the tunnel at flow velocity 35 m/s, sigma value 1 and incidence angle 3° .

the relative material resistance to cavitation erosion changes depending on the level of force applied to it. For low forces, material REF is less resistant than E. On the contrary, for higher forces above the intersection value, material REF is more resistant than E. Therefore, there exists the possibility that a different ranking could be obtained between both materials depending on the forces acting on them. Furthermore, it is clear that the equations from Table 2 permit to estimate the area of the pit provoked by any force level above the damaging threshold if it is assumed that the materials present the same linear behavior independently of the amplitude of the force.

On the other hand, the extremely high rate of events occurring on the hydrofoil under cavitation conditions has not permitted to monitor all the impulsive vibrations above the threshold level during the 75 h. Nevertheless, such difficulty has been overcome with a statistical study of the events estimated from discontinuous time segments as previously explained. This has required to perform a curve fit to link the distribution of lower force levels resulting from the *continuous measurements* with the higher ones resulting from the *triggered measurements*. As a result, the total distribution in the whole range of forces has been estimated with a power law regression. In particular, the histogram corresponding to the impulsive forces received by one specimen and its power law curve fit are shown on Figure 7. This result has been calculated considering that all the events have been uniformly distributed among the specimens, therefore it is supposed that only a quarter of the events monitored during the tests occur on a single specimen.

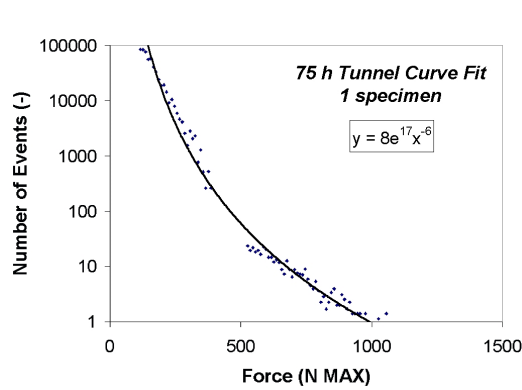


Figure 7: Curve fit of the histogram of inferred forces occurred on a single specimen during 75 h.

In order to estimate the damage induced by the collapse forces generated in the tunnel, the results obtained in the VCG have to be extrapolated to the higher range of force amplitudes now involved. In

the same way than before, each force has been associated to a proportional damage size. Then, all the estimated pit areas have been accumulated considering that no overlapping exists. Thus, a representative value of the total eroded area at the end of the tests has been obtained (Table 4) that can be compared with the experimental cavitation erosion data. A total eroded area of 1133 mm^2 is estimated for material REF against the 1889 mm^2 for material E. These results correlate with the relative volume loss measured on the specimens, 12 for REF against 70 for E (see Table 3). Both results indicate that in the tunnel tests the material E is weaker than the REF.

Material	Eroded Area (mm^2)
REF	1133.3
E	1888.6

Table 4: Total eroded area in mm^2 for materials REF and E, estimated after 75 h in the hydrodynamic tunnel.

Observing in detail the attacked area on the specimens, a narrow region is observed where most of the collapses concentrate which in turn is surrounded by a larger zone presenting a less intense attack. If no distinction is done between these two regions with different concentration of impingements, the total eroded area can be considered as about 280 mm^2 . As it is expected, the previous estimates presented in Table 4 are larger than these observations since no overlapping factor has been considered for them. The difference between observation and prediction can serve to estimate the approximate time from which the attacked area risks to be fully incubated. For instance, the minimum time estimated to fill a total eroded area of 280 mm^2 without pit overlapping is of 19 h for material REF and of 11 h for material E. Such prediction is confirmed with the visual observations carried out during the tests to control the evolution of the wear with time. It has been observed that after the first 10 h test the damage is already visible on the specimens. Therefore, the time predicted by this method would serve as an indicative of the expected time from which there is a risk of cavitation erosion.

5 Conclusions

Two different materials have been tested in a VCG in order to quantify their resistance to force intensities induced by single vortex cavity collapses. The intensity of the impact forces has been inferred from cavitation induced vibrations.

Based on the good linear regressions that have been obtained between maximum amplitude of forces above a well-defined damaging threshold and area of the pits, it has been assumed that the materials follow the same behavior for the range of forces occurring in the hydrodynamic tunnel which reach higher values than in the vortex generator.

Tests in a hydrofoil submerged in a water tunnel have been carried out to validate the previous results. The complex spatial and temporal distribution of vapor cavity collapses on the hydrofoil has been characterized with an adequate vibratory monitoring procedure combined with the use of two frequency response functions. So, the intensity and occurrence rate of cavitation collapses acting on the solid surface has been well estimated for a fixed hydrodynamic condition.

Finally, the application of the results obtained in the VCG to the forces measured in the hydrodynamic tunnel has permitted to estimate the relative resistance of the two materials and the extent of erosion on each specimen. These estimates correlate well with the relative volume loss measurements carried out on the tunnel specimens.

Summing up, the cavitation erosion predictions based on results obtained in the VCG are not in contradiction with the experimental cavitation erosion measurements on the hydrodynamic tunnel. Therefore, the current research work points towards the feasibility of the vibratory approach as a complete method for cavitation erosion prediction in hydraulic machinery if laboratory results are used. Nevertheless, further investigations are required because only two different materials have been tested for a single hydrodynamic condition in the tunnel. An extensive set of tests needs to be performed on various materials under different

flow conditions in order to clarify the uncertainties that still exist. To finish, it must be reminded that the next step is to apply this technique to actual machines.

Acknowledgements

The authors would like to thank the Fonds pour projets et études de l'économie électrique (PSEL Foundation) and Sulzer Innotec AG for their financial support. The experimental research was carried out in the LMH-IMHEF Laboratories (EPFL Lausanne) within the Cavitation Group. Thanks are also given to the CUR (Generalitat de Catalunya) for their grant.

References

- Avellan, F., Henry, P. and Rhyning, I. L. (1987), *A New High Speed Cavitation Tunnel for Cavitation Studies in Hydraulic Machinery*, Proc. of ASME Annual Meeting, Boston (USA).
- Bourdon, P. (2000), *La Détection Vibratoire de l'Érosion de Cavitation des Turbines Francis*, Ph.D. Thesis, EPFL, Switzerland.
- Escaler, X., Dupont, P. and Avellan, F. (1999), *Experimental Investigation on Forces due to Vortex Cavitation Collapse For Different Materials*, *Wear* 233-235, pp. 65-74.
- Escaler, X. (2000), *A Vibratory Approach to Cavitation Erosion Prediction*, Ph.D. Thesis, UPC, Spain.
- Farhat, M. and Avellan, F. (1988), *Shock Pressure Generated by Cavitation Vortex Collapse*, Symposium on Cavitation Noise and Erosion in Fluid Systems, ASME Annual Meeting, San Francisco.
- Karimi, A. and Avellan, F. (1986), *Comparison of Erosion Mechanisms in Different Types of Cavitation*, *Wear* 133, pp. 305-322.
- Kaye, M. (1999), *Cavitation Monitoring of Hydraulic Machines by Vibration Analysis*, Ph.D. Thesis, EPFL, Switzerland.
- Quang, L. (1984), *Étude Physique du Comportement des Poches de Cavitation Partielle*, Ph.D. Thesis, INPG, France.